Latin American Journal of Solids and Structures
www.lajss.org

Failure Analysis of Polypropylene Fiber Reinforced Concrete Two-Way Slabs Subjected to Static and Impact Load Induced by Free Falling Mass

Abstract

The impact resistance of concrete is considered as poor due to a relatively energy dissipating characteristics and tensile strength. Therefore, this paper investigates the feasibility of using polypropylene fibers (PF) to enhance punching shear capacity of reinforced concrete (RC) two-way slabs subjected to drop-weight impacts. The evaluated parameters included two slab thickness (70 mm and 90 mm), five different PF percentages (0%, 0.3%, 0.6%, 0.9%, and 1.2%), and two impact load height (1.2 m and 2.4 m). The tested slabs divided into three groups: not subjected to impact load, subjected to impact load at a height of 1.2 m, and subjected to impact load at a height of 2.4 m, resulting in a total of 25 slabs. The behavior of each two-way RC slab was evaluated in terms of the crack patterns, ultimate punching shear capacity. The present experimental data can be used for further assessment of the performance of PF reinforced concretes two-way slabs as well as providing a well-documented dataset related to the impact-resistant applications which is presently limited within the literature. The results showed that adding the PF at a dosage of 0.3 to 1.2% by volume of concrete and increasing the slab thickness from 70 mm to 90 mm leads to considerable enhancement in the overall structural behavior of the slabs and their resistance to impact loading. Interestingly, the degradation in the ultimate punching capacity of the slabs subjected to impact load at a height of 1.2 and 2.4 m is 30.5% and 34.6%, respectively. Finally, an empirical model was proposed for predicting the punching shear capacity of RC two-way slabs based on reliable experimental results available in literature

Keywords

Post Behavior; Impact Resistance; Polypropylene Fiber; Reinforced Concrete; Two-Way Slabs.

Rajai Z. Al-Rousan[a]*

[a] Department of Civil Engineering, Jordan University of Science and Technology, Irbid, Jordan, Email: rzalrousan@just.edu.jo

*Corresponding author

http://dx.doi.org/10.1590/1679-78254895

Received: February 04, 2018
In Revised Form: February 22, 2018
Accepted: February 22, 2018
Available online: March 19, 2018

1 INTRODUCTION

The response of reinforced concrete (RC) elements subjected to impact load is a hot topic in the previous published research work and still needs more elaboration in order to understand their complex behavior. This hot topic is very important especially in the area of RC nuclear facilities or military

fortification structures that are used in high-hazard or high-threat applications as well as in the structures that are designed to resist the accidental impact loading due to falling rock and ship or vehicle collisions with offshore facilities, bridges, and buildings. Therefore, an extensive work should be undertaken in an attempt to develop a design procedure for post impact resistant and to improve the behavior of RC elements subjected to impact loads. Up to now, the developing of empirical provisions for estimating the damage and structural capacity under specific impact loading is the most focused topic of the majority of the impact loading related research (Kennedy (1976), Vimal et al. (2017), Wei et al. (2013), Chen and May (2009)). Furthermore, more of the research work has been exclusively focused on slab and wall mechanism of localized damage such as impactor penetration, concrete scabbing, and impactor perforation (Chang-Geun et al. (2015), Duc-Kien and Seung-Eock (2014), Shujian et al. (2016)). In addition, little effort is focused on the energy dissipation due to damage growth at localized location and global deformations in terms of axial, shear and bending deformations of RC flat slabs under impact loading (Duc-Kien and Seung-Eock (2017)). Nowadays two-way RC flat slabs can be consider as the superlative solution for residential, commercial, and office buildings because of the efficient and economical issues such as easy installation of electrical and mechanical infrastructures, the greatly simpler and reduced formwork, and faster site operations as well as the easier and versatility space partitioning. Moreover, the punching failure can be considered as a complex behavior in design of the RC two-way flat slab. In addition, the punching failure is typically brittle and considered as ultimate load capacity of two-way RC slabs and can cause a sudden collapses of the entire structure (Lorena et al. (2016)). The bent-up bars, closed stirrups, post-installed shear reinforcement or shear studs techniques as well as high strength concrete are used to increase the punching shear capacity of RC two-way flat slabs (Micael et al. (2015)).

Recently, utilization of fiber reinforced concrete (FRC) has emerged as a practical approach for enhancing the performance of RC elements under impact loading. Numerous studies have shown FRC elements containing conventional steel reinforcing bars demonstrate superior resistances to global impact behavior than local damage mechanism development and, as a result, acquire enhanced energy absorption capabilities under impact loading with respect to RC elements (Ong et al. (1997), Kurihashi et al. (2006), Zhang et al. (2007)). In addition, FRC is used to increase the punching shear capacity and the deformation capacity of RC flat slabs due to the capability of fibers in the bridging after the creation of the cracks (Cheng and Parra-Montesinos (2010), Maya et al. (2012)).

Current design code provisions (ACI 318-14 (2014), Fédération Internationale du Béton-Vol. 1 (2010a), Fédération Internationale du Béton-Vol. 2 (2010b), JSCE (2007)) for punching shear had been proposed for normal weight concrete structures and their appliance to for FRC flat slab is not constantly straightforward especially for empirical design formula. Over the last decades, several stipulated empirical models for punching shear of FRC flat slab have been proposed by taking into account the contribution of tensile and compressive strength at the critical section of the punching shear as well as the pull out strength and quantity of fibers (Choi et al. (2007), Higashiyama et al. (2011), ASTM (2004)). Base d on the previous literature review, the punching shear strength of the RC two-way flat slabs after impact load is omitted. Therefore, this paper presents the methodology and conclusions from an experimental program undertaken to study the effect of impact load on the punching shear behavior of RC and polypropylene fiber reinforced (PFR) concrete two-way slabs. Highlighting was placed on assessing the effect of slab thicknesses, fiber volume fractions, and freely dropped weight heights on the RC two-way flat slab behavior in terms of ultimate load capacity, deflection profile, toughness or energy absorption as well as mode of failure. In an effort to fully detain the post impact behaviors of the tested RC slabs, the test data collected were used to propose an analytical formula that can estimate the pre impact and post impact punching shear capacity of RC flat two-way slabs with and without PFR.

2 DESCRIPTION OF EXPERIMENTAL PROGRAM

2.1 Test specimens

The experimental program included testing twenty eight two-way reinforced concrete slabs as simply supported system with equal clear length and width of 1.0 m as shown in Figure 1. The investigated parameters include the slab thicknesses, h_s (7 cm and 9 cm), fiber volume fractions, V_f (0%, 0.3%, 0.6%, 0.9%, and 1.2%), and freely drop weight (10 cm in diameter and weighs 7 kg) heights, h_l (1.2 m and 2.4 m). The slabs were reinforced with seven steel bars with a diameter of 5 mm in each direction which is equivalent to steel reinforcement ratios of 0.0018 and 0.0025 for the 9 cm and 8 cm slabs according to the ACI 318-14 Code (2014). A dropped mass height of 1.2 m and 2.4 m produces impact velocity of 4.85 m/s and 6.86 m/s, respectively, as well as kinetic energy of 82.32 J and 164.64 J, respectively.

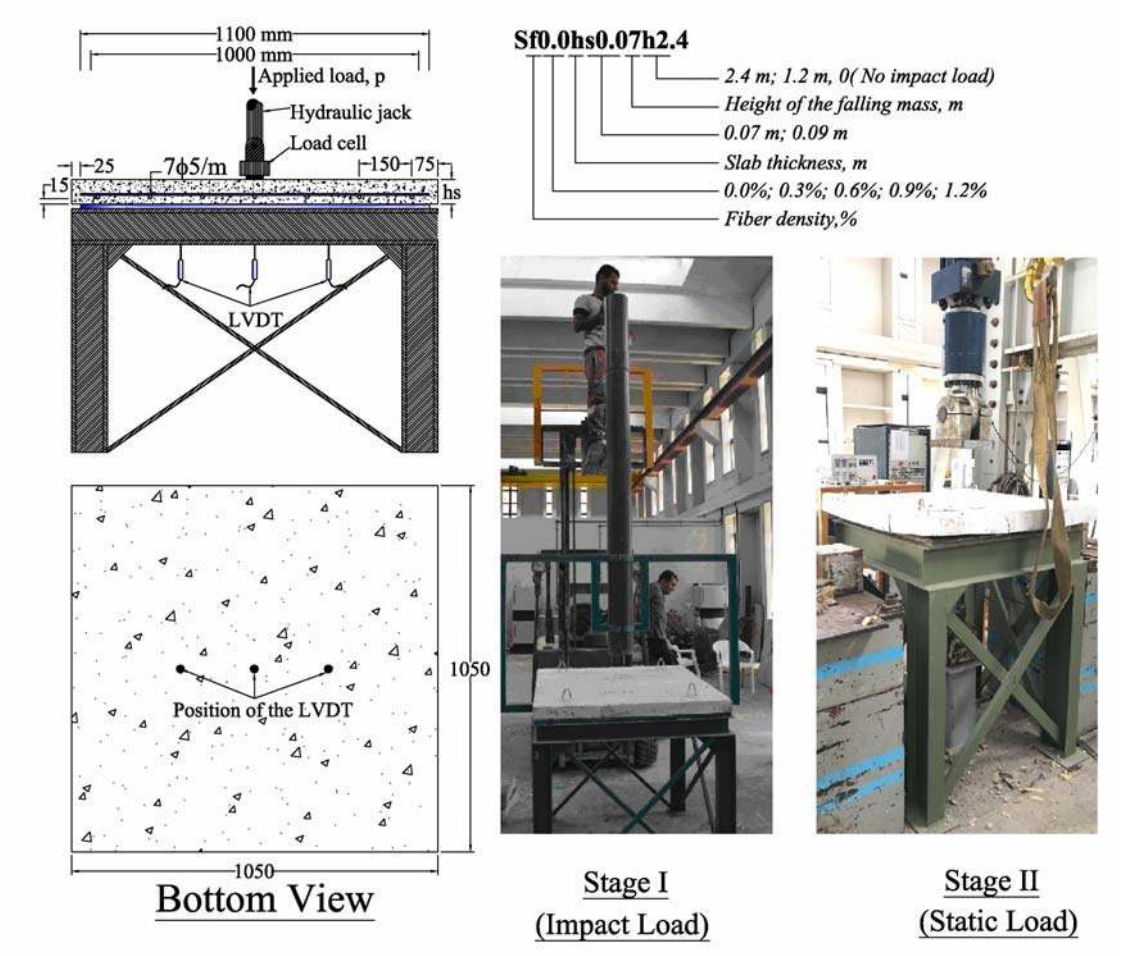

Figure 1: *Tested slabs layout and setup details (all dimensions in mm).*

2.2 Concrete Mixture

The mixture ingredients include Type I ordinary cement (375 kg/m^3), local coarse aggregate (916 kg/m^3), local fine aggregate (700 kg/m^3), and silica sand (64 kg/m^3). The specific gravities for the coarse and fine aggregates were 2.5 and 2.6, respectively. Polypropylene fibers with a monofilament configuration were used with a length of 19 mm, tensile strength of 165 MPa, specific gravity of 0.91,

excellent alkali resistance, ability in decreasing drying and plastic shrinkage, ability in increasing impact resistance of young concrete, ability to reinforced concrete by acting mechanically with multi-dimensional fiber network coated with mortar. All the ingredients were mixed consistently and then the fibers were feeding manually to ensure the uniform distribution of fibers in the concrete mixture as shown in Figure 2. Then the concrete is placed in the wooden molds, vibrating them, straightening the top of the concrete specimen, de-molding the specimens for 24 hours after casting, and placing the specimens in lime-saturated water for 28 days for curing.

Figure 2: *Mixing procedure of the tested two way slab*

2.3 Test Setup and Instrumentation

The RC two-way slabs were tested firstly under impact load (A steel ball of 7 kg mass with adjustable heights of 1.2 m to 2.4 m is allowed to fall freely through 150 mm in diameter hollow tube member placed vertically to stick the top surface of the tested two way slabs at the center) by using a special design setup consists of steel members with I-section joined together to provide a horizontal platform to give simply supported condition for the two way slab as shown in Figure 1 (Stage 1). Then, all slabs were loaded up to failure using a hydraulic jack centrally positioned at the top of the slab as shown in Figure 1 (Stage 2). The reference slabs that have not subjected to impact load were just loaded up to failure (Stage 2). A square steel plate with a thickness of 50 mm and a side length of 200 mm was used to simulate the a column with 200 mm sides as shown in Figure 1. The applied load was measured by using load cell and three linear variable differential transformers (LVDT) were placed at specific location to measure the deflection profile of the tested slabs as shown in Figure 1.

3 RESULTS AND DISCUSSION

3.1 Concrete Strength Results

Figure 3 shows the stress-strain diagrams for the concrete with different fiber volume fractions as well as the compressive strength, splitting tensile strength, and modulus of elasticity. Inspection of

Figure 3 reveals that the slope of the stress-strain curve is linear up (young's modules of elasticity) to about 30–40% of the ultimate compressive strength, after that the curves become non-linear due to the initiation of the micro cracks at the paste-aggregate interface. The ultimate stress occurred after the formulation of the large crack within the concrete. Also, Figure 3 shows that the maximum compressive strength (f'_c), splitting tensile strength (f_r), and young's modules of elasticity (E_c) increased with the increase of the increasing of polypropylene content according to ASTM-C39, ASTM C496, and ASTM-C469 (ASTM (2004)), respectively. The results also show that the polypropylene fibers had higher effect on the tensile strength and dynamic modules of elasticity than the compressive strength.

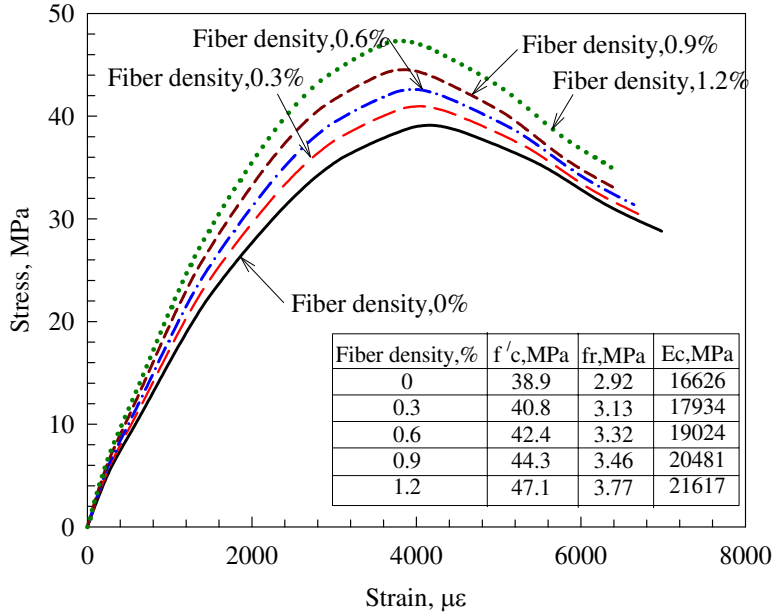

Fiber density,%	f 'c,MPa	fr,MPa	Ec,MPa
0	38.9	2.92	16626
0.3	40.8	3.13	17934
0.6	42.4	3.32	19024
0.9	44.3	3.46	20481
1.2	47.1	3.77	21617

Figure 3: *Stress-strain diagrams and mechanical properties of concrete (f'_c : compressive strength, f_r : splitting tensile strength, and E_c : young's modules of elasticity)*

3.2 Analysis of Failure Mode and Ultimate Load Capacity

Based on the experimental results, all tested slabs were failed in the punching shear mode and flexural cracks started from the loading steel plate and extended until the edges of the tested slab. Punching shear mode or failure was brittle failure which occurred near the loading steel plate (compression face or top surface) at the ultimate failure load, followed by the development of a punching shear failure cone at the tensile face (Bottom surface). Figures 4-6 show the typical punching shear failure on the compression face and tensile face. Inspection of Figure 4 reveals that the 90 mm slab thickness had a remarkable impact on the flexural cracks and punching shear cone than 70 mm slab thickness by decreasing the number of the flexural cracks (Tensile face) and small punching shear cone. Also, Figure 5 shows that slabs subjected to impact had more flexural cracks and large punching shear cone than slabs not subjected to impact. In addition, Figure 6 shows the increasing of fiber volume decreased the number of flexural crack and the size of punching shear cone because the fibers contribution in the resisting of the applied forces until the fibers were pulled out from the concrete. Additionally, the occupation of fibers in stretching the failed bottom surface (tension face) of the slab away from the loading steel plate thus increased their punching shear capacity.

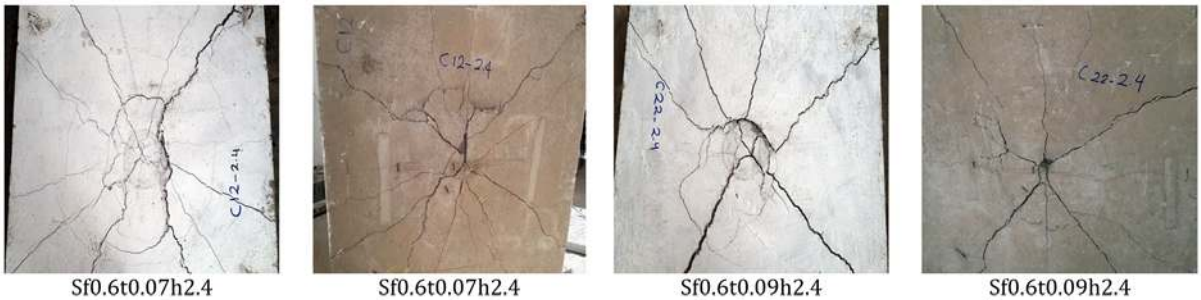

Figure 4: *Effect of slab thickness on crack patterns*

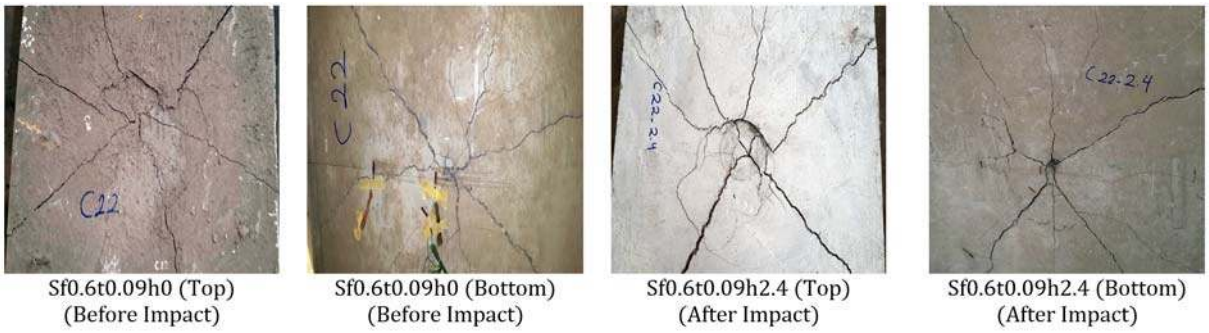

Figure 5: *Effect of impact load on crack patterns*

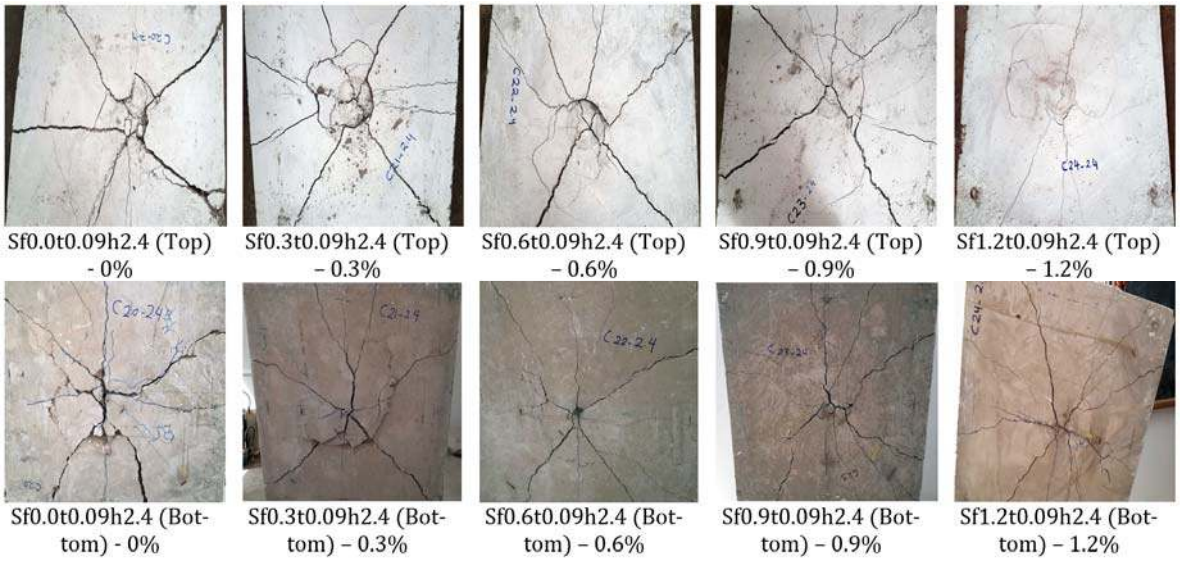

Figure 6: *Effect of fiber volume on crack patterns*

Table 1: *Specimens' Details and Test Results*

Slab	Percent of fibers by volume (V_f)	Slab thickness (h_s), m	Height of the falling mass (h_I), m	Ultimate punching shear load (V_R), kN	Toughness, kN.mm
Sf0.0t0.07h0	0	0.07	None	88.9	1588
Sf0.3t0.07h0	0.30%			93.4	1852
Sf0.6t0.07h0	0.60%			96.1	2094
Sf0.9t0.07h0	0.90%			100.7	2470
Sf1.2t0.07h0	1.2%			108.4	2859
Sf0.0t0.09h0	0	0.09		120.1	2169
Sf0.3t0.09h0	0.30%			126.1	2519
Sf0.6t0.09h0	0.60%			128.8	2671
Sf0.9t0.09h0	0.9%			135.3	3076
Sf1.2t0.09h0	1.20%			144.8	3410
Sf0.0t0.07h1.2	0	0.07	1.2	61.8	1432
Sf0.3t0.07h1.2	0.30%			67.8	1768
Sf0.6t0.07h1.2	0.60%			74.9	2028
Sf0.9t0.07h1.2	0.90%			83.0	2335
Sf1.2t0.07h1.2	1.2%			91.0	2616
Sf0.0t0.07h2.4	0	0.07	2.4	58.1	1339
Sf0.3t0.07h2.4	0.30%			63.9	1658
Sf0.6t0.07h2.4	0.60%			70.4	1982
Sf0.9t0.07h2.4	0.90%			77.9	2285
Sf1.2t0.07h2.4	1.2%			85.5	2528
Sf0.0t0.09h2.4	0	0.09		80.7	1813
Sf0.3t0.09h2.4	0.30%			88.9	2203
Sf0.6t0.09h2.4	0.60%			94.0	2526
Sf0.9t0.09h2.4	0.90%			105.2	2932
Sf1.2t0.09h2.4	1.2%			116.6	3367

Note: Toughness is defined as the area under the load versus deflection curve

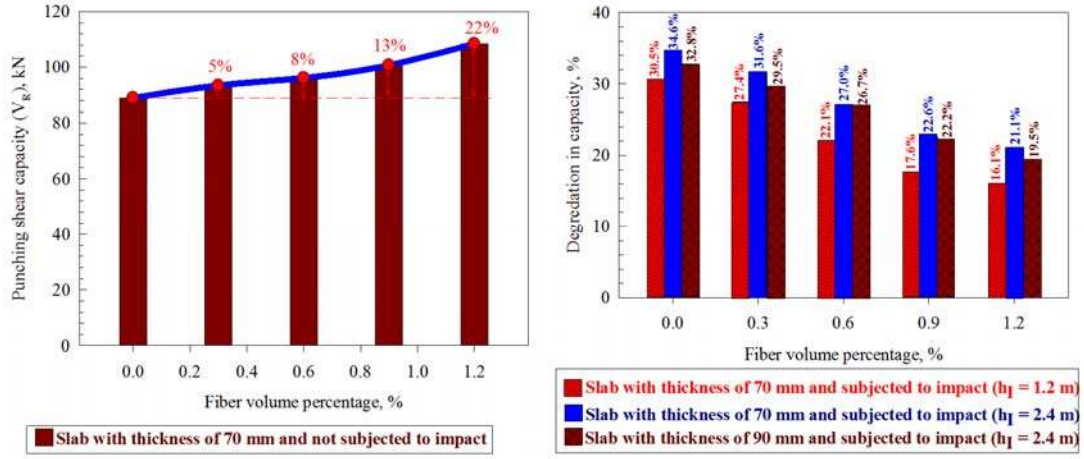

Figure 7: *Effect of fiber volume percentage and impact load on punching shear load*

Table 1 and Figure 7 show the summarized results and the effect of fiber volume percentage and impact load on punching shear load of the tested slabs. Inspection of Figure 7 reveals that the ultimate punching shear capacity of control slab (slabs not subjected to impact) generally increases and the degradation in slab strength due to impact load decreases with the increasing fiber volume percentage. Adding PFR in 0.3 to 1.2% by volume fraction increased the ultimate punching capacity with respect to slab without PFR by about 5 to 22%, respectively. While, the slab thickness (h_s = 90 mm) has a strong impact on the ultimate punching shear capacity with an enhancement of 35% with respect to slab with a thickness of 70 mm. In addition, the impact load at a height of 1.2 m and 2.4 m created degradation in the ultimate punching shear capacity of 30.5% and 34.6%, respectively, as well as the efficiency of fiber in absorbing of impact load or decreasing the ultimate load capacity degradation (30.5% to 16.1%) is increased with the increasing of PFR percentage.

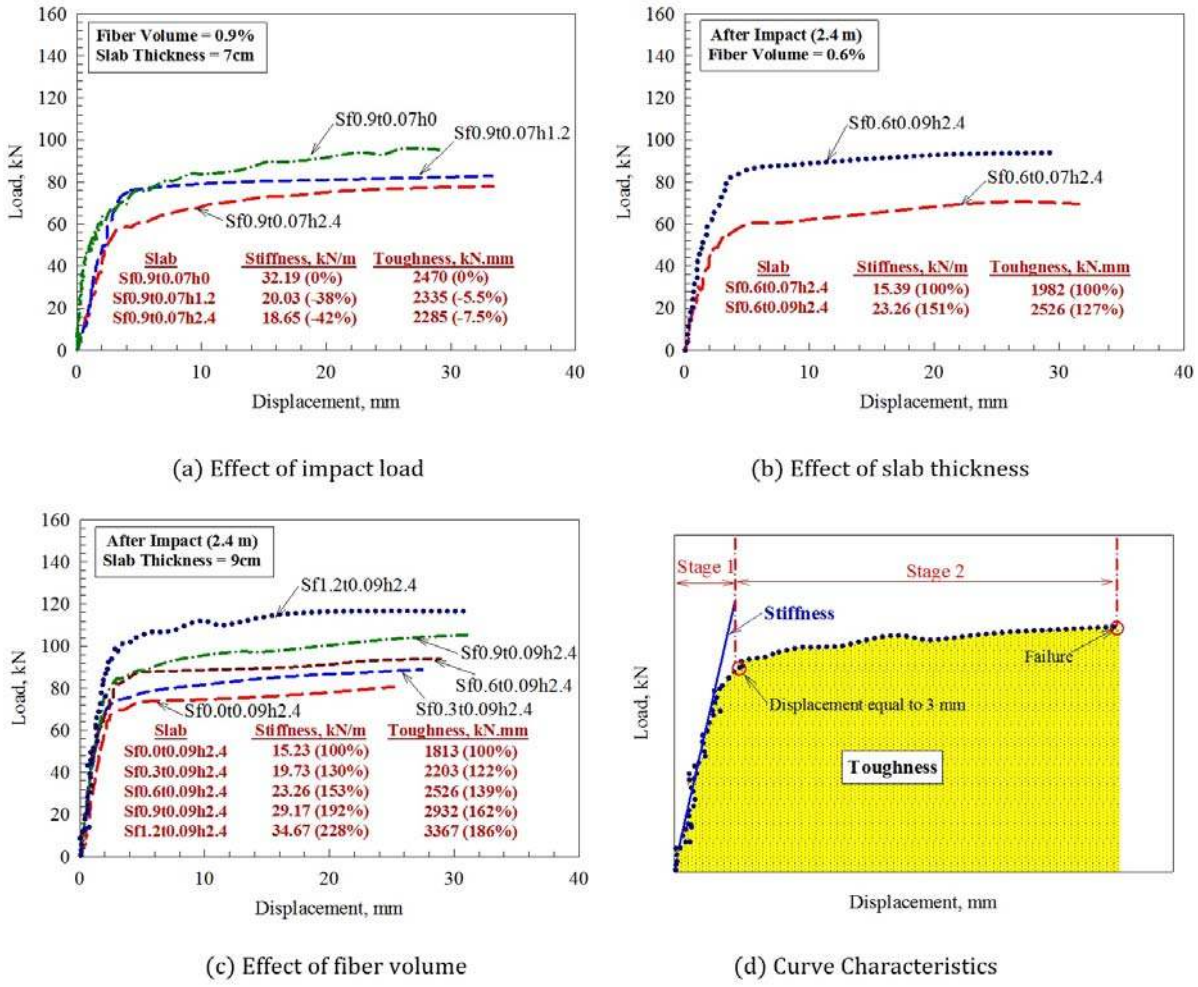

Figure 8: *Typical load versus displacement curves*

3.3 Load Deflection Behavior

Figure 8 (a-c) shows the effect of the impact load, slab thickness, and fiber volume on the load displacement behavior, stiffness, and toughness. The stiffness is defined as the slope of the part between the initiation of the first crack (reaching the tensile strength of the concrete) and the load at

which the displacement equal to 3 mm and the toughness is defined as the area under the load displacement behavior. The load displacement behavior can be divided into two stages based on the crack growth and the shape of the load-displacement behavior as shown in Figure 8(d). In the first stage (zero loading to load at which the displacement equal to 3 mm), the behavior is approximately elastic liner before the initiation of the first crack (which is located at the center of slab and close to the loading steel plate) which is caused a reduction in the stiffness of the curve. Then, in the second stage, the stiffness was reduced suddenly, followed by the development of the punching shear cone. Inspection of Figure 8(a) reveals that the impact load at a height of 1.2 m and 2.4 m caused a reduction of 3.8% and 4.2%, respectively, in stiffness and 5.5% and 7.5%, respectively, in toughness with respect to control slab (no impact load). While, the slab thickness (h_s = 90 mm) has a helpful strong impact on the stiffness and toughness with an enhancement of 151% and 127%, respectively, with respect to slab with a thickness of 70 mm as shown in Figure 8(b). In addition, Figure 8(c) shows that the stiffness and toughness generally increase (30% to 128%) and (22% to 86%), respectively, with the increasing fiber volume percentage (0.3% to 1.2%) because adding PFR assist to delay and resist the formulation and expanding of cracks, thus slab stiffness and toughness are enhanced.

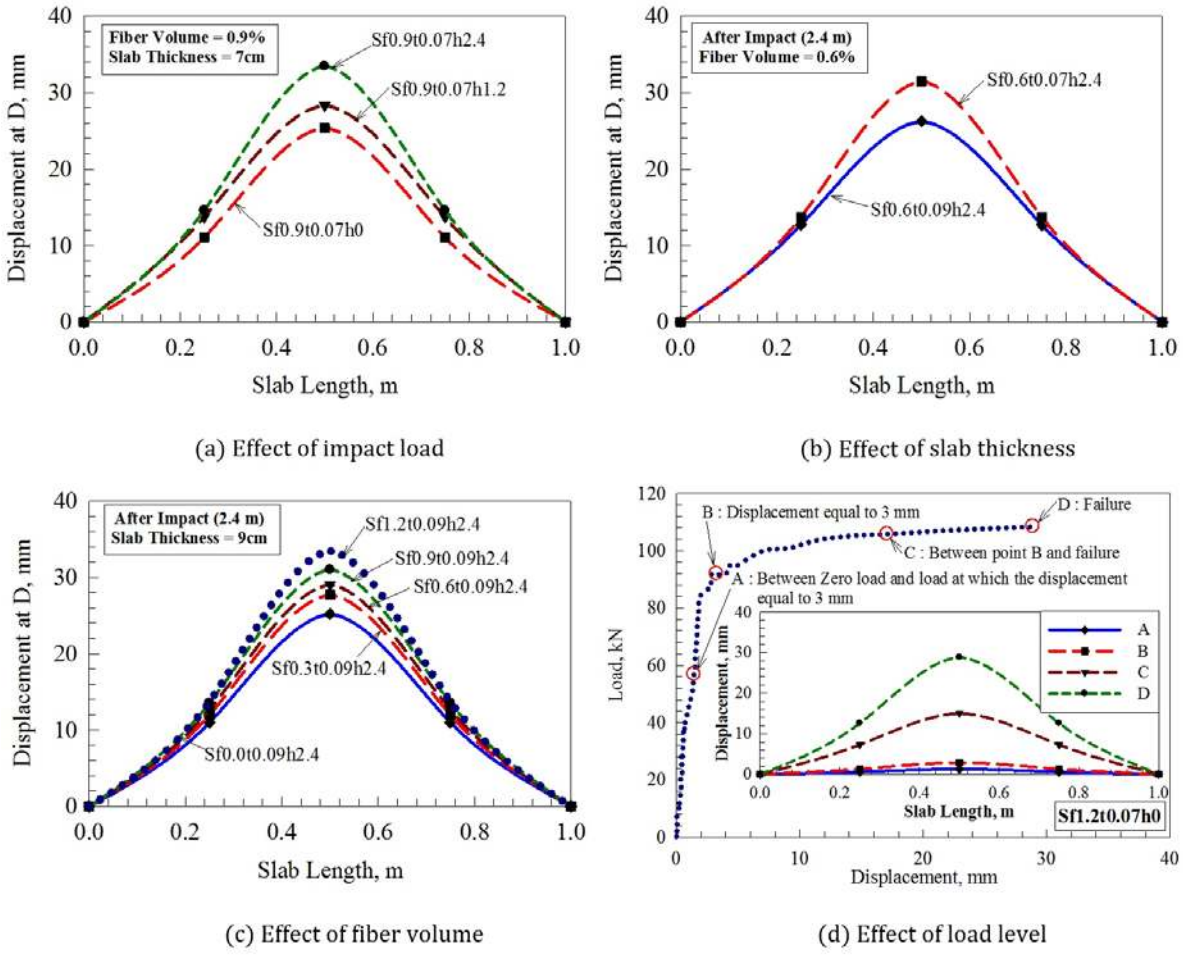

Figure 9: *Typical displacement shapes*

3.4 Deflection Profile

Assessment of the displacement profile of the tested slabs provides further information (quantitative measure) on the topic of the effect of tested parameters (Figure 9) on the global structural behavior that is not directly obvious from studying of the load-displacement behavior and ultimate mid-point displacement. Figure 9 (a-c) shows the effect of the impact load, slab thickness, and fiber volume on the displacement profile. While Figure 9 (d) shows the displacement profile at different load value (A: point between zero load and the load at which the displacement equal to 3 mm; B: point at displacement equal to 3 mm; C: point between the B and failure point; and D: point at failure at ultimate punching load capacity. Inspection of Figure 9(a) reveals that the impact load at a height of 2.4 m had the highest displacement profile specifically at the mid-point comparing with impact load at a height of 1.2 m. This conclusion is observed the same in the mode of failure where that slabs subjected to impact at a height of 2.4 had more flexural cracks and large punching shear cone than slabs subjected to impact at a height of 1.2 m. While the displacement at the quarter-point is almost equal for both impact heights. In addition the slab thickness had the same effect on the displacement profile (mid-point and quarter-point) as the impact load and decreased with the increasing of the slab thickness as shown in Figure 9(b). In comparing all of the displacement profile showed in Figure 9(c), it can be seen that the PFR were successful in justifying the growth of localized failures in terms of number of flexural crack and the size of the punching shear cone, the PFR slabs exhibited displacement profile in which displacement were more consistently distributed and, as a result, were able to achieve larger displacement profile at failure.

4 EMPIRICAL MODEL

4.1 Punching Shear Model for Two-Way RC Slabs Subjected to Impact Load

Prediction of punching shear strength in RC two-way slabs with different slab thicknesses, fiber volume fractions, and freely drop weight heights (Impact load) is fundamental in order to propose structural design procedures for structures subjected to impact load. Thus, an empirical model was proposed to predict the punching shear strength of two-way RC slabs subjected to impact load as a function of tested parameters. Most models founded in the literature and design codes base their verifications on a critical section to find the punching shear strength of non-impacted RC slabs without shear reinforcement (Lorena et al. (2016), Micael et al. (2015), Ong et al. (1997), Kurihashi et al. (2006), Zhang et al. (2007), Cheng and Parra-Montesinos (2010), Maya et al. (2012), ACI Committee 318 (2014), Fédération Internationale du Béton (FIB-Vol. 1) (2010a), Fédération Internationale du Béton (FIB-Vol. 2) (2010b), JSCE (2007), Choi et al. (2007), Higashiyama et al.(2011), ASTM (2004), Selcuk and Frank (2009)). Eq. (1) shows the ACI 318-14 (2014) expression for circular or square columns of two way slab moderate relative to the concrete compressive strength and thickness of the slab

$$V_R = 0.33 b_o d \sqrt{f_c'} \tag{1}$$

where V_R is the punching shear capacity of two-way slabs at critical section located at d/2 from the face of the square or circular column. d is the effective depth of the slab, f′c is the concrete compressive strength at 28 days, and b_o is the perimeter of the critical section. Based on the above equation, Eq. (2) can be used to describe the punching shear capacity of RC two-way slabs subjected to impact with some modifications as following:

$$V_R = \alpha \beta b_o d \sqrt{f_c'} \tag{2}$$

where α and β is a factor accounting for fiber volume fraction and impact load effects, respectively. Based on the regression analysis of the RC two-way slabs not subjected to impact load (β = 1) (Figure 10), Eq. (3) presents the relationship between the fiber volume fraction and α factor.

$$\alpha = 0.321\, e^{0.1523\, V_f} \tag{3}$$

where V_f is the fiber volume fraction percentage. Based on the regression analysis of the RC two-way slabs subjected to impact load at a height of 1.2 and 2.4 m which is equivalent to a kinetic energy (KE) of 82.32 J and 164.64 J, respectively, (Figure 11), Eq. (4) and (5) presents the relationship between the fiber volume fraction and β factor, respectively.

$$\beta = 0.700e^{0.172V_f} \quad \text{for} \quad \text{KE} = 82.32\,\text{J} \tag{4}$$

$$\beta = 0.664e^{0.16V_f} \quad \text{for} \quad \text{KE} = 164.64\,\text{J} \tag{5}$$

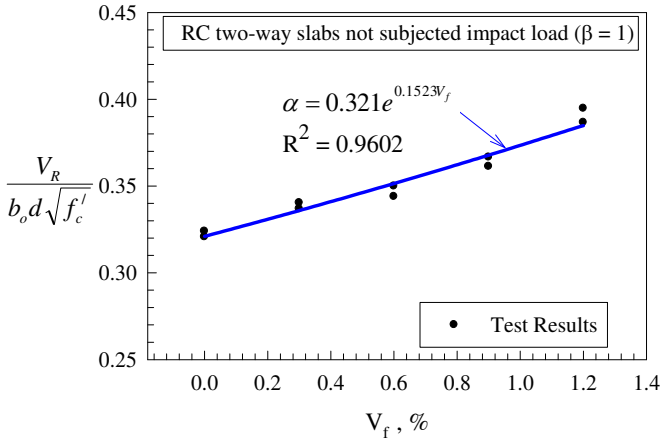

Figure 10: *Relationships between fiber volume fraction percentage (V_f) and α factor for RC two way slabs not subjected impcat load*

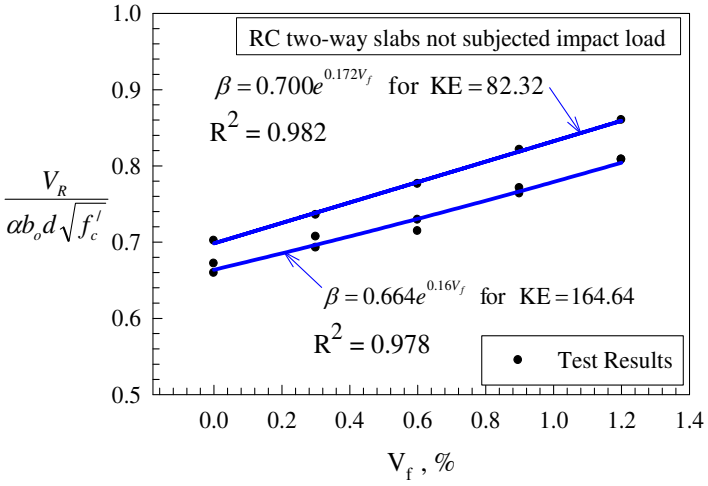

Figure 11: *Relationships between fiber volume fraction percentage (V_f) and β factor for RC two way slabs subjected impcat load*

Thus the punching shear strength of the RC two-way slabs subjected to impact can be defined by the following equations

$$V_R = \left(0.321\, e^{0.1523\, V_f}\right) b_o d \sqrt{f_c'} \quad \text{for KE} = 0 \text{ (No impact)} \tag{6}$$

$$V_R = \left(0.213\, e^{0.3123\, V_f}\right) b_o d \sqrt{f_c'} \quad \text{for KE} = 82.32 \text{ J} \tag{7}$$

$$V_R = \left(0.225\, e^{0.324\, V_f}\right) b_o d \sqrt{f_c'} \quad \text{for KE} = 164.64 \text{ J} \tag{8}$$

Table 2: *Existing Punching Shear Strength Models*

Authors	Punching Shear Strength Model
Narayanan and Darwish (1987)	$V_R = \left(0.24 f_{sp} + 16\rho + 0.41\tau_b a_f \frac{l_f}{d_f}\right)\left(1.6 - 0.002 h_s\right)\left(1 - 0.55 V_f a_f \frac{l_f}{d_f}\right)\left(4e + 3\pi h_s\right)$ $a_f = \begin{cases} 0.5 & \text{for round fibers} \\ 0.75 & \text{for crimped fibers} \\ 1.0 & \text{for duoform fibers} \end{cases}$
Shaaban and Gesund (1994)	$V_R = 0.6\left(0.25\left(3.27 V_f\right) + 0.567\right)\left(4\left(e + d\right)\right)\left(d\right)\left(\sqrt{f_c'}\right)$
Harajli et al. (1995)	$V_R = \left(0.33 + 0.075 V_f\right)\left(4\left(e + d\right)\right)\left(d\right)\left(\sqrt{f_c'}\right)$
Higashiyama et al. (2011)	$V_R = \left(\beta_d\right)\left(\beta_p\right)\left(\beta_r\right)\left(f_{pcd} + \left(0.41\tau_b V_f a_f \frac{l_f}{d_f}\right)\right)\left(e + \pi d\right)\left(1 - 0.32 V_f a_f \frac{l_f}{d_f}\right)\left(d\right)$ $f_{pcd} = 0.2\sqrt{f_c'} < 1.2MPa,\ \beta_d = \sqrt[4]{\frac{1000}{d}} < 1.5,\ \beta_p = \sqrt[3]{100\rho} < 1.5$ $\beta_r = 1 + \frac{1}{1 + 0.25\left(e/d\right)}$
Present Study	$V_R = \left(0.321 e^{0.1523 V_f}\right)\left(4\left(e + d\right)\right)\left(d\right)\left(\sqrt{f_c'}\right)$

Note: where f_{sp} is the indirect cylinder tensile strength of fiber reinforced concrete, $\tau_b = 4.15$ MPa is the average fiber-matrix interfacial bond stress, α_f is a factor depending of the fiber geometry, l_f is the length of the fiber, d_f is the diameter of the fiber, V_f is the volume of the fiber, d is the effective depth of the slab, e is the column side length, ρ is the steel reinforcement ratio, and f'_c is the concrete compressive strength at 28 days

Table 3: *Predicted to test punching shear strength*

Slab	V_R, kN					
	Tested	Narayanan and Darwish (1987)	Shaaban and Gesund (1994)	Harajli et al. (1995)	Higashiyama et al. (2011)	Present Study
Sf0.0t0.07h0	88.9	96.8	93.4	90.6	113.5	88.1
Sf0.3t0.07h0	93.4	100.2	97.4	96.8	123.5	92.2
Sf0.6t0.07h0	96.1	103.6	101.5	102.9	132.9	96.5
Sf0.9t0.07h0	100.7	106.8	105.5	109.1	141.7	101.1

Sf1.2t0.07h0	108.4	109.9	109.5	115.3	149.9	105.8
Sf0.0t0.09h0	120.1	144.8	127.4	123.5	162.0	120.2
Sf0.3t0.09h0	126.1	150.0	132.9	132.0	176.3	125.8
Sf0.6t0.09h0	128.8	155.0	138.4	140.4	189.8	131.7
Sf0.9t0.09h0	135.3	159.8	143.9	148.8	202.3	137.8
Sf1.2t0.09h0	144.8	164.4	149.4	157.2	214.0	144.3
Predicted/Test		1.123	1.049	1.063	1.397	0.999
Coefficient of variation		0.061	0.017	0.027	0.051	0.014
Correlation Coefficient		0.978	0.995	0.993	0.991	0.997

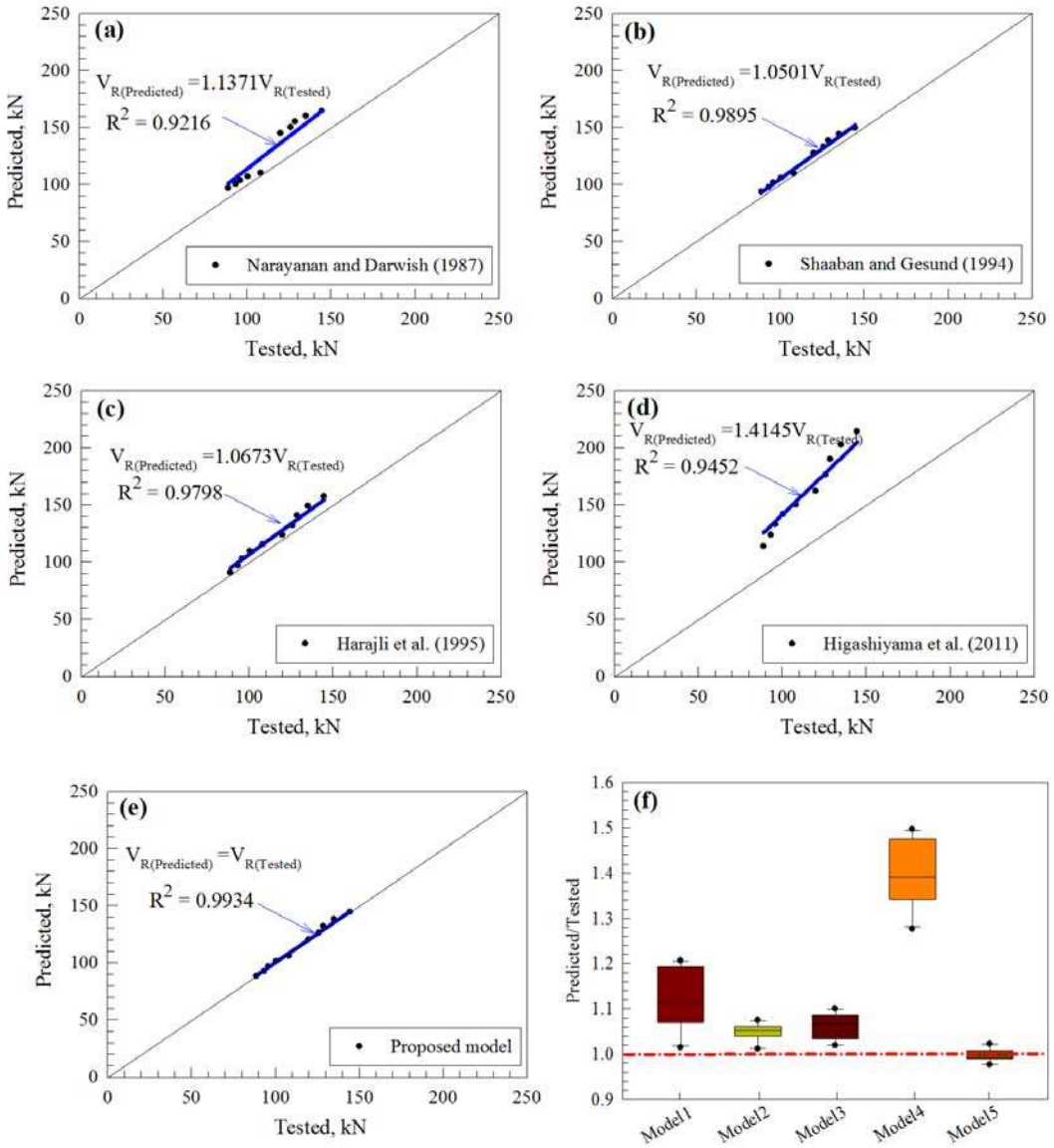

Figure 12: *Tested punching shear strength versus predicted of existing models (Model1: Narayanan and Darwish (1987); Model2: Shaaban and Gesund (1994); Model3: Harajli et al. (1995); Model4: Higashiyama et al. (2011); Model5: Present Study)*

4.2 Predictability of Various Theoretical Models

To find the predictability and the accuracy of the proposed model in Eq. (6), it was compared with the punching shear models which are the most valid and accurate model for proposed model (Narayanan and Darwish (1987); Shaaban and Gesund (1994); Harajli et al. (1995); Higashiyama et al. (2011)) as shown in Table 2. The average value (predicted/tested), coefficient of variation and correlation coefficient for punching shear capacity predicted by using various theoretical models are shown in Table 3. Inspection of Table 3 reveals that the predicted value Shaaban and Gesund (1994) and Harajli et al. (1995) is closed to the tested value with an average value (predicted/tested) of 1.049 and 1.063, respectively, as well as the correlation coefficients are more than 0.95 which reflects that the behavior of the test data are well described by these models. Also, Narayanan and Darwish (1987) have an acceptable (predicted/tested) of 1.123. While, Higashiyama et al. (2011) is overestimated the punching shear capacity with an average value of 1.397. Figure 12 shows the tested punching shear strength versus predicted of existing models. Inspection of Figure 12(a-d) reveals that the theoretical models are overestimated the punching shear strength of the tested slabs with higher R^2 more than 90%. In addition, Figure 12(f) shows that the proposed model provides the highest number of predictions of (predicted/tested) in the intervals [0.98-1.02] and the Higashiyama et al. (2011) have the lowest number of predictions of (predicted/tested) in the intervals [1.28-1.49].

4.3 Predictability of the Proposed Model

The proposed model is checked against published experimental results by predicting the punching shear strength as shown in Table 4. In addition, the average value (predicted/tested), coefficient of variation and correlation coefficient for the experimental results presented by Theodorakopoulos and Swamy (1993), Alexander and Simmonds (1992)], Swamy and Ali (1982), Harajli et al. (1995), Narayanan and Darwish (1987), and Higashiyama et al. (2011)] are summarized in Table 4. Inspection of Table 4 reveals that the average prediction error ranged from 2% for Theodorakopoulos and Swamy (1993) to 37% for Narayanan and Darwish (1987), where the average value and the Correlation Coefficient for all the experimental results was approximately equal 87% and 94%, respectively, which shows that the proposed model has a good prospective to predict punching shear strength

5 CONCLUSIONS

Based on the results and observations, the following conclusions are drawn:

1. The increasing in slab thickness had a notable effect on the flexural cracks and punching shear cone by decreasing the number of the flexural cracks (Tensile face) and the size of punching shear cone while the increasing in impact load and the fiber volume are increased the number of the number of flexural cracks and the size of punching shear cone.
2. The increasing in slab thickness of 28% had an enhancement of the ultimate punching shear capacity of 35% and the adding PFR in 0.3 to 1.2% by volume fraction enhanced the ultimate punching capacity with 5 to 22% while the impact load at a height of 1.2 m and 2.4 m created degradation in the ultimate punching shear capacity of 30.5% and 34.6%.
3. The impact load caused a reduction of less than 10% in stiffness and toughness of the tested slabs but the slab thickness enhanced the stiffness and toughness with an enhancement of 151% and 127%, respectively, as well as the stiffness and toughness increased (30% to 128%) and (22% to 86%), respectively, with the increasing fiber volume percentage of 0.3% to 1.2%.
4. The PFR slabs exhibited displacement profile in which displacement were more consistently distributed and, as a result, were able to achieve larger displacement profile at failure.
5. The proposed empirical model was in good agreement with theoretical models experimental results available in literature in predicting the ultimate punching shear capacity of two way slabs not subjected to impact.

Table 4: *Literature Experimental data and punching shear strength prediction*

Specimen	h, mm	d, mm	e, mm	f_c', MPa	ρ, %	V_f, %	V_{exp}, kN	$V_{Predicted}$, kN	$\frac{V_R(\text{Predicted})}{V_R(\text{Tested})}$
Theodorakopoulos and Swamy (1993)									
FS-1	125	100	150	35.4	0.56	0.00	173.5	191	1.10
FS-2	125	100	150	34.0	0.56	0.50	225	202	0.90
FS-3	125	100	150	35.6	0.56	1.00	247.4	223	0.90
FS-4	125	100	150	35.7	0.56	1.00	224.4	223.3	1.00
FS-5	125	100	150	38.0	0.37	1.00	198.1	230.4	1.16
FS-6	125	100	150	35.7	0.37	1.00	174.5	223.3	1.28
FS-7	125	100	150	36.6	0.37	1.00	192.4	226.1	1.18
FS-19	125	100	150	34.5	0.37	0.00	136.5	188.5	1.38
FS-20	125	100	150	37.0	0.37	1.00	211	227.4	1.08
FS-8	125	100	100	36.7	0.56	0.00	150.3	155.6	1.04
FS-9	125	100	100	35.6	0.56	1.00	216.6	178.4	0.82
FS-10	125	100	200	36.4	0.56	0.00	191.4	232.4	1.21
FS-11	125	100	200	34.2	0.56	1.00	259.8	262.3	1.01
FS-12	125	100	150	36.1	0.56	1.00	217.5	224.6	1.03
FS-13	125	100	150	33.5	0.56	1.00	235.5	216.4	0.92
FS-14	125	100	150	35.0	0.56	1.00	239.5	221.1	0.92
FS-15	125	100	150	31.2	0.56	1.00	238	208.8	0.88
FS-16	125	100	150	27.9	0.56	1.00	227.8	197.4	0.87
FS-17	125	100	150	46.8	0.56	1.00	268.4	255.7	0.95
FS-18	125	100	150	14.2	0.56	1.00	166	140.9	0.85
Alexander and Simmonds (1992)									
P11F0	155	132.7	200	33.2	0.5	0.00	257.0	326.6	1.27
P11F31	155	132.7	200	35.8	0.5	0.39	324.0	359.9	1.11
P11F66	155	132.7	200	35.0	0.5	0.84	345.0	381.1	1.10
P38F0	155	105.7	200	38.1	0.63	0.00	264.0	256.1	0.97
P38F34	155	105.7	200	38.4	0.63	0.43	308.0	274.5	0.89
P38F69	155	105.7	200	38.5	0.63	0.88	330.0	294.4	0.89
Swamy and Ali (1982)									
S-1	125	100	150	37.80	0.56	0.00	197.7	197.4	1.00
S-2	125	100	150	39.00	0.56	0.60	243.6	219.6	0.9
S-3	125	100	150	37.80	0.56	0.90	262.9	226.3	0.86
S-4	125	100	150	36.90	0.56	1.20	281.0	234.1	0.83
S-5	125	100	150	37.80	0.56	0.90	267.2	226.3	0.85
S-6	125	100	150	38.00	0.56	0.90	239.0	226.9	0.95
S-7	125	100	150	38.90	0.74	0.00	221.7	200.2	0.90
S-13	125	100	150	39.30	0.74	0.90	236.7	230.8	0.98

S-12	125	100	150	36.80	0.74	0.90	249.0	223.3	0.90
S-11	125	100	150	37.10	0.74	0.90	262.0	224.2	0.86
S-8	125	100	150	41.10	0.74	0.90	255.7	236.0	0.92
S-16	125	100	150	38.90	0.56	0.90	213.0	229.6	1.08
S-10	125	100	150	38.90	0.46	0.90	203.0	229.6	1.13
S-9	125	100	150	38.90	0.37	0.90	179.3	229.6	1.28
S-19	125	100	150	38.90	0.37	0.00	130.7	200.2	1.53
Harajli et al. (1995)									
A1	55	39	100	29.60	1.12	0.00	58.8	37.9	0.64
A2	55	39	100	30.00	1.12	0.45	63.6	40.8	0.64
A3	55	39	100	31.40	1.12	0.80	73.1	44.1	0.60
A4	55	39	100	24.60	1.12	1.00	64.7	40.2	0.62
A5	55	39	100	20.00	1.12	2.00	58.3	42.2	0.72
B1	75	55	100	31.40	1.12	0.00	91.8	61.3	0.67
B2	75	55	100	31.40	1.12	0.45	105.9	65.7	0.62
B3	75	55	100	31.80	1.12	0.80	108.4	69.7	0.64
B4	75	55	100	29.10	1.12	1.00	108.8	68.8	0.63
B5	75	55	100	29.20	1.12	2.00	134.5	80.2	0.60
Narayanan and Darwish (1987)									
S1	60	45	100	43.3	1.84	0.00	86.50	55.1	0.64
S2	60	45	100	52.1	1.84	0.25	93.40	62.8	0.67
S3	60	45	100	44.7	1.84	0.50	102.00	60.4	0.59
S4	60	45	100	46.0	1.84	0.75	107.50	63.7	0.59
S5	60	45	100	53.0	1.84	1.00	113.60	71.0	0.63
S6	60	45	100	53.0	1.84	1.25	122.20	73.8	0.60
S7	60	45	100	47.0	1.6	1.00	92.60	66.9	0.72
S8	60	45	100	45.3	2.08	1.00	111.10	65.7	0.59
S9	60	45	100	43.5	2.3	1.00	111.30	64.3	0.58
S10	60	45	100	47.6	2.53	1.00	111.30	67.3	0.60
S11	60	45	100	29.8	1.84	1.00	82.10	53.3	0.65
S12	60	45	100	32.4	1.84	1.00	84.90	55.5	0.65
Higashiyama et al. (2011)									
t100-0.67	100	70	100	24.6	0.85	0.67	137.50	83.9	0.61
t140-0.67	140	110	100	24.6	0.54	0.67	210.20	162.9	0.78
t180-0.67	180	150	100	24.6	0.4	0.67	297.60	264.5	0.89
t100-0.72	100	65	100	42.4	0.91	0.72	140.80	100.1	0.71
t140-0.72	140	105	100	42.4	0.57	0.72	213.20	200.8	0.94
t180-0.72	180	145	100	42.4	0.41	0.72	290.70	331.4	1.14
t100-0.91	100	65	100	21.6	0.91	0.91	120.80	73.5	0.61
t140-0.91	140	105	100	21.6	0.57	0.91	183.10	147.5	0.81
t180-0.91	180	145	100	21.6	0.41	0.91	231.20	243.5	1.05

t100-0.63	100	70	100	27.8	0.85	0.63	152.30	88.7	0.58
t100-0.94	100	70	100	31.1	0.85	0.94	147.90	98.3	0.66
t100-1.03	100	70	100	30.4	0.85	1.03	158.90	98.6	0.62

Summary

Authors	Predicted/Test	Coefficient of variation	Correlation Coefficient
Theodorakopoulos and Swamy (1993)	1.02	0.15	0.64
Alexander and Simmonds (1992)	1.04	0.14	0.53
Swamy and Ali (1982)	1.00	0.19	0.55
Harajli et al. (1995)	0.64	0.06	0.99
Narayanan and Darwish (1987)	0.63	0.07	0.87
Higashiyama et al. (2011)	0.78	0.24	0.97
All	0.87	0.26	0.94

Acknowledgement

The authors acknowledge the technical support provided by the Jordan University of Science and Technology (JUST).

References

ACI Committee 318. (2014) Building code requirements for structural concrete (ACI 318–014) and commentary (ACI 318R–14). Farmington Hills (MI): American Concrete Institute.

Alexander SDB, Simmonds SH. (1992) Punching shear tests of concrete slab–column joints containing fiber reinforcement. ACI Structure Journal; 89(4): 425–32.

ASTM standards construction: (2004) Concrete and aggregates (V. 04-05). MI, USA: American Society for Testing Materials.

Chang-Geun Cho, Andreas J. Kappos, Hyung-Joo Moon, Hyun-Jin Lim. (2015) Experiments and failure analysis of SHCC and reinforced concrete composite slabs. Engineering Failure Analysis; 56(1): 320-331.

Chen, Y., and May, I. M. (2009) Reinforced Concrete Members under Drop Weight Impacts. Proceedings of the Institution of Civil Engineers. Structures and Buildings; 162(1): 45-56.

Cheng MY, Parra-Montesinos GJ. (2010) Evaluation of steel fiber reinforcement for punching shear resistance in slab–column connections – Part I: Monotonically increased load. ACI Structure Journal; 107(1): 101–9.

Choi K, Reda Taha M, Park H, Maji A. (2007) Punching shear strength of interior concrete slab–column connections reinforced with steel fibers. Cement Concrete Compos; 29(5): 409–20.

Narayanan R. and Darwish IYS. (1987) Punching shear tests on steel fibre reinforced micro-concrete slabs. Magazine of Concrete Research; 39(138): 42–50.

Duc-Kien Thai, Seung-Eock Kim. (2014) Failure analysis of reinforced concrete walls under impact loading using the finite element approach. Engineering Failure Analysis; 45(1): 252-277.

Duc-Kien Thai, Seung-Eock Kim. (2017) Numerical simulation of pre-stressed concrete slab subjected to moderate velocity impact loading. Engineering Failure Analysis; 79(1): 820-835

Fédération Internationale du Béton (FIB). (2010a) Model Code 2010 – first complete draft, vol. 1, Fédération Internationale du Béton, Bulletin 55. Lausanne (Switzerland).

Fédération Internationale du Béton (FIB). (2010b) Model Code 2010 – first complete draft, vol. 2, Fédération Internationale du Béton, Bulletin 55. Lausanne (Switzerland).

Harajli MH, Maalouf D, Khatib H. (1995) Effect of fibers on the punching shear strength of slab–column connections. Cement Concrete Compos; 17 (2): 161–70.

Higashiyama H, Ota A, Mizukoshi M. (2011) Design equation for punching capacity of SFRC slabs. International Journal of Concrete Structures and Materials; 5(1): 35–42.

JSCE. (2007)Standard specifications for concrete structures-2007, Design. Tokyo (Japan): Japan Society of Civil Engineers.

Kennedy, R. P. (1976)A Review of Procedures for the Analysis and Design of Concrete Structures to Resist Missile Impact Effects. Nuclear Engineering and Design; 37(2): 183-203.

Kurihashi, Y.; Taguchi, F.; Kishi, N.; and Mikami, H. (2006) Experimental Study on Static and Dynamic Response of PVA Short-Fiber Mixed RC Slab. fib Proceedings of the 2nd International Congress, ID 13-20, Naples, Italy, 10 pp.

Lorena Francesconi, Luisa Pani,Flavio Stochino. (2016) Punching shear strength of reinforced recycled concrete slabs. Construction and Building Materials; 127: 248–263

Maya L.F., Fernández Ruiz, Muttoni A., Foster S.J. (2012) Punching shear strength of steel fibre reinforced concrete slabs. Engineering Structures; 40(1): 83–94.

Micael M. G. Inácio, André F. O. Almeida, Duarte M. V. Faria, Válter J. G. Lúcio, António Pinho Ramos. (2015) Punching of high strength concrete flat slabs without shear reinforcement. Engineering Structures; 103: 275–284.

Ong, K. C. G.; Basheerkhan, M.; and Paramasivam, P. (1997) Behavior of Fiber-Reinforced Concrete Slabs under Low Velocity Projectile Impact. High Performance Concrete Proceedings: ACI International Conference, Malaysia, SP-172, V. M. Malhotra, ed., American Concrete Institute, Farmington Hills, MI: 993-1011.

Selcuk Saatci and Frank J. Vecchio. (2009) Nonlinear Finite Element Modeling of Reinforced Concrete Structures under Impact Loads. ACI Structural Journal; 106(5): 717-725.

Shaaban AM. Gesund H. (1994) Punching shear strength of steel fiber reinforced concrete flat plates. ACI Structure Journal; 91(4): 406–414.

Shujian Yao, Duo Zhang, Xuguang Chen, Fangyun Lu, Wei Wang. (2016) Experimental and numerical study on the dynamic response of RC slabs under blast loading. Engineering Failure Analysis; 66(1): 120-129.

Swamy RN, Ali SAR. (1982) Punching shear behavior of reinforced slab–column connections made with steel fiber concrete. ACI Structure Journal; 79(6): 392–406.

Theodorakopoulos DD, Swamy N. (1993) Contribution of steel fibers to the strength characteristics of lightweight concrete slab–column connections failing in punching shear. ACI Structure Journal; 90(4): 342–55.

Vimal Kumar, M.A. Iqbal, A.K. Mittal (2017). Experimental investigation of prestressed and reinforced concrete plates under falling weight impactor, Thin-Walled Structures; ISSN 0263-8231, https://doi.org/10.1016/j.tws.2017.06.028.

Wei Wang, Duo Zhang, Fangyun Lu, Song-chuan Wang, Fujing Tang. (2013). Experimental study and numerical simulation of the damage mode of a square reinforced concrete slab under close-in explosion. Engineering Failure Analysis; 27(1): 41-51

Zhang, J.; Maalej, M.; and Quek, S. T. (2007) Performance of Hybrid- Fiber ECC Blast/Shelter Panels Subjected to Drop Weight Impact. Journal of Materials in Civil Engineering, ASCE; 19(10): 855-863.